Pure appl. geophys. 155 (1999) 443–470
0033–4553/99/040443–28 $ 1.50 + 0.20/0

© Birkhäuser Verlag, Basel, 1999

Pure and Applied Geophysics

Precursory Seismic Quiescence before the 1994 Kurile Earthquake ($M_w = 8.3$) Revealed by Three Independent Seismic Catalogs

KEI KATSUMATA[1] and MINORU KASAHARA[1]

Abstract—We have found that the $M_w = 8.3$ Kurile earthquake on October 4, 1994 followed an outstanding seismic quiescence starting 5–6 years before the mainshock near the ruptured area. We have analyzed three independent seismic catalogs: Institute of Seismology and Volcanology, Hokkaido University (ISV), Japan Meteorological Agency (JMA) and International Seismology Center (ISC). In spite of selecting different magnitude bands and time windows all three catalogs presented the common feature of the seismic quiescence. This fact strongly suggests that the seismic quiescence should not be a man-made change but actually occurred. Moreover we have confirmed that the seismic quiescence was the most significant and the earthquake was the largest in the past twenty-five years in this region. Therefore we confidently interpret this seismic quiescence as an indication of a preparation process for the $M_w = 8.3$ Kurile earthquake.

Key words: Seismicity pattern, seismic quiescence, Kurile, Hokkaido Toho-Oki, earthquake prediction.

1. Introduction

The Kurile Islands (Hokkaido Toho-Oki) earthquake ($M_w = 8.3$) occurred on October 4, 1994 in the southern part of the Kurile Islands (Fig. 1). The focal mechanism was not a low-angle thrust-type, the centroid depth was large and the stress drop was high (KIKUCHI and KANAMORI, 1995; TANIOKA *et al.*, 1995). The azimuth and the dip of the aftershock area were most probably parallel to the trench axis and near vertical, respectively (KATSUMATA *et al.*, 1995; FURUKAWA, 1995). Coseismic crustal deformations were clearly consistent with the vertical fault plane (TSUJI *et al.*, 1995; OZAWA, 1996). These facts strongly suggest that this event is a lithospheric earthquake: an intra-plate event that ruptures through a substantial part of the subducting oceanic lithosphere (KIKUCHI and KANAMORI, 1995).

Many authors have reported that precursory seismic quiescences occurred in and around focal areas several years before earthquakes: Tonga-Kermadec (WYSS *et al.*, 1984), Tokachi-Oki (MOGI, 1969; HABERMANN, 1981b), Oaxaca (OHTAKE *et*

[1] Institute of Seismology and Volcanology, Graduate School of Science, Hokkaido University, Sapporo, Japan, 0600810. E-mail: katsu@eos.hokudai.ac.jp

al., 1977; HABERMANN, 1981b; MCNALLY, 1981), Aleutians (HABERMANN, 1981a; KISSLINGER, 1988), Lima (HABERMANN, 1981a), Colima (HABERMANN, 1981b; MCNALLY, 1981), Hawaii (WYSS *et al.*, 1981; WYSS, 1986), Hokkaido (TAYLOR *et al.*, 1991), Kuriles (HABERMANN, 1981b), Morgan Hill (HABERMANN and WYSS, 1984), San Andreas (WYSS and BURFORD, 1985, 1987; WYSS and HABERMANN, 1988), Landers (WIEMER and WYSS, 1994) and Izu-Oshima (WYSS *et al.*, 1996). TAKANAMI *et al.* (1996) have found a seismic quiescence starting three years before the $M_w = 8.3$ Kurile mainshock in 1994. Their analysis was based on an earthquake catalog produced by ISV.

To confirm the results of TAKANAMI *et al.* (1996), we have analyzed three different catalogs compiled by not only ISV but also both JMA and ISC. These institutions independently locate hypocenters and estimate magnitudes. If seismic quiescences have actually occurred in an area, they should be detected by different seismic catalogs. An apparent change in seismicity rate is easily brought on by artificial reasons: deployment of new seismic stations, closing of old seismic stations, changes in seismograph, waveform recording system and magnitude estimation algorithm (HABERMANN, 1987, 1991). Therefore, to compare the results from the three seismic catalogs provides us with evidence to verify whether or not a seismic quiescence detected in a target area is a fact.

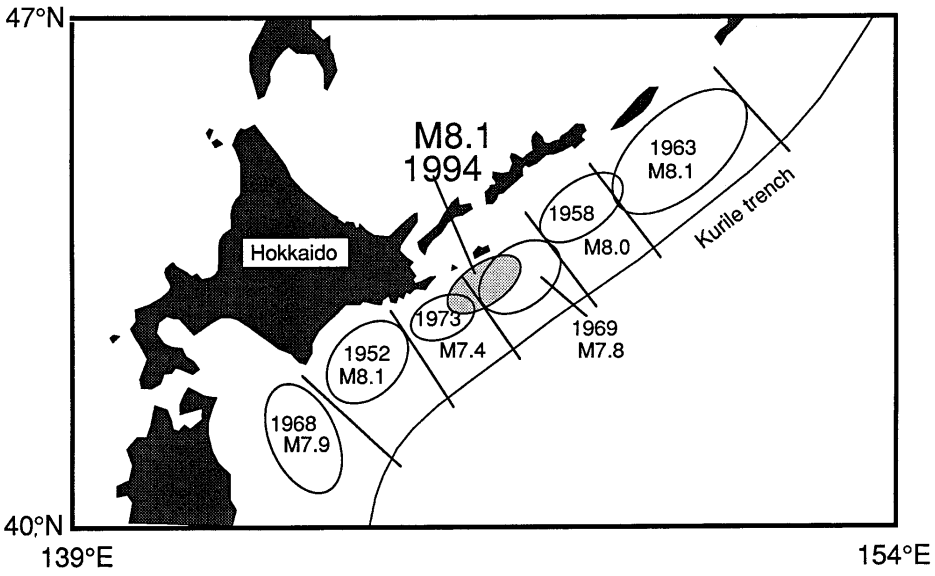

Figure 1
Great earthquakes off the coast of Hokkaido and off the southern Kurile Islands. JMA determined magnitudes. Ellipses roughly show each aftershock area.

Table 1

Characteristic parameters used in this study for the ISV, the JMA and the ISC seismic catalog

	ISV	JMA	ISC
Target area	144–149°E 42–44.5°N	144–149°E 42–44.5°N	144–149°E 42–44.5°N
Time window	1 March, 1985– 3 October, 1994	1 January, 1977– 3 October, 1994	1 January, 1970– 3 October, 1994
Length of time window (days)	3504	6485	9042
Magnitude	$M \geq 3.0$	$M \geq 4.3$	$M \geq 5.0$
Depth (km)	0–150	0–150	0–150
Number of earthquakes (original)	1445	946	526
Number of earthquakes (declustered)	1390	491	336

2. Data

Table 1 summarizes key parameters of the data used in this study. Details of each seismic catalog are described below.

2.1 ISV

ISV operates a regional seismic network called Hokkaido Seismic Network which consists of about thirty stations in Hokkaido and the northern part of the Honshu Islands. A typical station consists of three seismometers in a vault, i.e., one vertical and two horizontal (north-south and east-west) components, with a natural frequency of 1 Hz, amplifiers with magnifications of 30 to 72 dB and 10 or 16 bits analogue-to-digital converters. All waveform data are telemetered continuously to ISV in Sapporo by dedicated telephone lines of Nippon Telephone and Telegram Company. ISV started the field installation of the network in 1976 and finished it in 1985. Moreover thirty-one short-period seismic stations deployed by Japan Meteorological Agency (JMA) were added to the Hokkaido Seismic Network in 1997. A drastic change in the data processing system of ISV occurred on 20 May, 1993. Before the day, arrival times of P- and S-waves were read on seismograms from a 24-channel pen recorder with a paper speed of 1 cm/s and magnitudes were determined at each station using the following equation,

$$M_{F-P} = 2.75 \log T_{F-P} - 2.24, \tag{1}$$

where M_{F-P} is magnitude and T_{F-P} is time in seconds measured from the arrival time of P-waves to the time when the amplitudes of the coda of S-waves return to

the ground noise level. M_{F_P}s at some stations were averaged to obtain the representative magnitude of an event.

In 1993 the WIN system running on a UNIX workstation (URABE and TSUKADA, 1992) was installed at ISV. WIN is a powerful tool to show waveform data on a computer display, to read manually arrival times and maximum amplitudes, to calculate the hypocenter using HYPOMH (HIRATA and MATSU'URA, 1987) and to show a seismicity map. Magnitudes are determined at each station using the following equation (WATANABE, 1971),

$$0.85M_A - 2.50 = \log Av + 1.73 \log r \quad (r < 200 \text{ km}), \tag{2}$$

where M_A is a magnitude, Av is the maximum velocity amplitude in cm/s on the vertical component and r is the epicentral distance in km. Therefore, the ISV catalog includes two different magnitudes estimated using (1) and (2). That is the reason why a magnitude shift and stretch occurred in 1993.

From the original seismic catalog of ISV, hypocenters with more than five P-wave and one S-wave readings were selected for relocation in a rectangular area (144–149°E, 42–44.5°N). First, we calculated hypocenters using HYPOMH (HIRATA and MATSU'URA, 1987) without station corrections and plotted residuals vs. epicentral distances for each station. Since the residuals were found to shift linearly as a function of epicentral distance, a straight line was fitted using the least-squares method. We obtained station corrections as a function of epicentral distance for each seismic station. Then the station corrections were added to arrival times and hypocenters relocated using HYPOMH.

After the relocation of hypocenters we made a correction for the magnitude change in 1993 in the target area of this study. The b-values were estimated to be 1.4 and 0.8 for a period between 1 March, 1985 and 20 May, 1993 (Period of old system) and a period between 20 May, 1993 and 3 October, 1994 (Period of new system), using events larger than $M = 3.5$ and 3.0, respectively. In this magnitude band the seismicity rate in Period of new system decreased to 0.4 compared to that in Period of old system. This is caused by the drastic shift and stretch of magnitude. Thereafter we assumed that the background seismicity rate and b-value in Period of old system was the same as that in Period of new system. We, derived the equation:

$$M_{\text{new}} = 1.83M_{\text{old}} - 3.45,$$

where M_{old} is a magnitude in Period of old system and M_{new} is the corresponding magnitude in Period of new system. Note that this equation is available for events with $M_{\text{old}} = 3.5$ and larger.

After the correction, we plotted the number of earthquakes vs. magnitude in the study area to estimate the magnitude of completeness, M_c. The algorithm we use interprets the point of the peak in the (non-cumulative) frequency-magnitude

distribution as M_c. We concluded that all events larger than $M = 3.0$ were reported homogeneously between 1 March, 1985 and 3 October, 1994, that is, $M_c = 3.0$. 1445 earthquakes larger than $M = 3.0$ which occurred from 1 March, 1985 to 3 October, 1994 were selected in the area between 144.0–149.0°E and 42.0–44.5°N. Earthquakes were selected with depths between 0 and 150 km beyond the depth of 60–70 km at which the seismic fault of the mainshock extended, because the seismicity change should be estimated not only on the seismic fault but also in its surrounding portion. Figure 2a shows epicenters including clustered events.

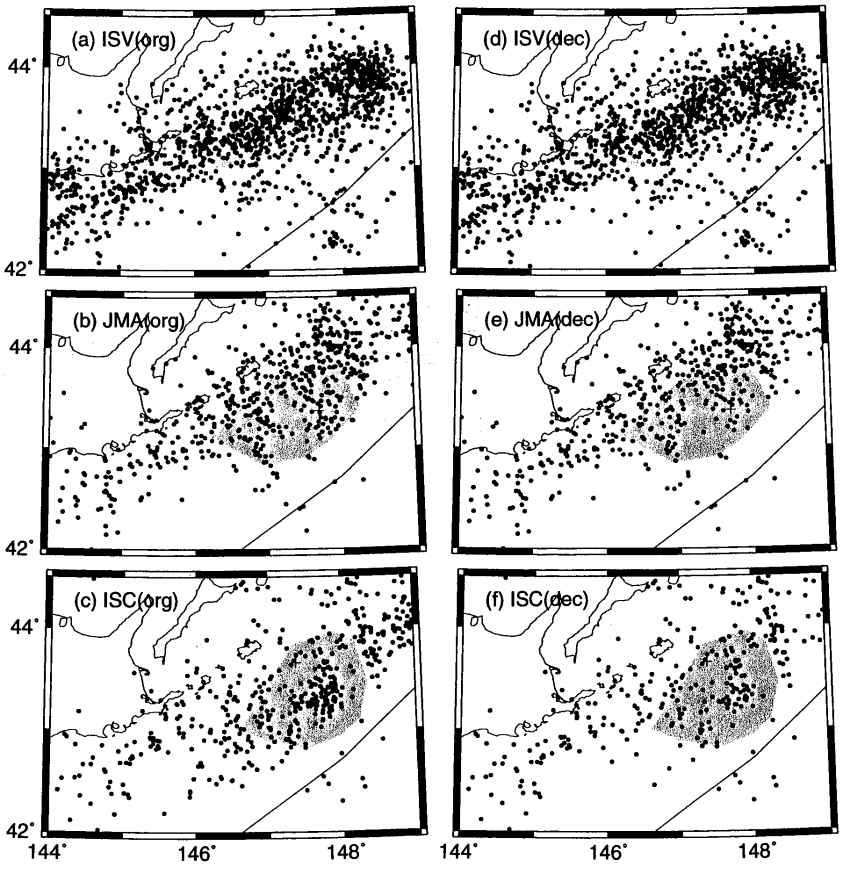

Figure 2
Epicenters of earthquakes used in this study. Hatched areas show the aftershock area of the 1994 Kurile earthquake, which are estimated using each catalog. (a)–(c) are original catalogs of ISV (1 March, 1985–3 October, 1994, $M \geq 3.0$), JMA (1 January, 1977–3 October, 1994, $M \geq 4.3$) and ISC (1 January, 1970–3 October, 1994, $M \geq 5.0$), respectively. (d)–(f) are declustered catalogs, excluding aftershocks and earthquake swarms from the original catalogs.

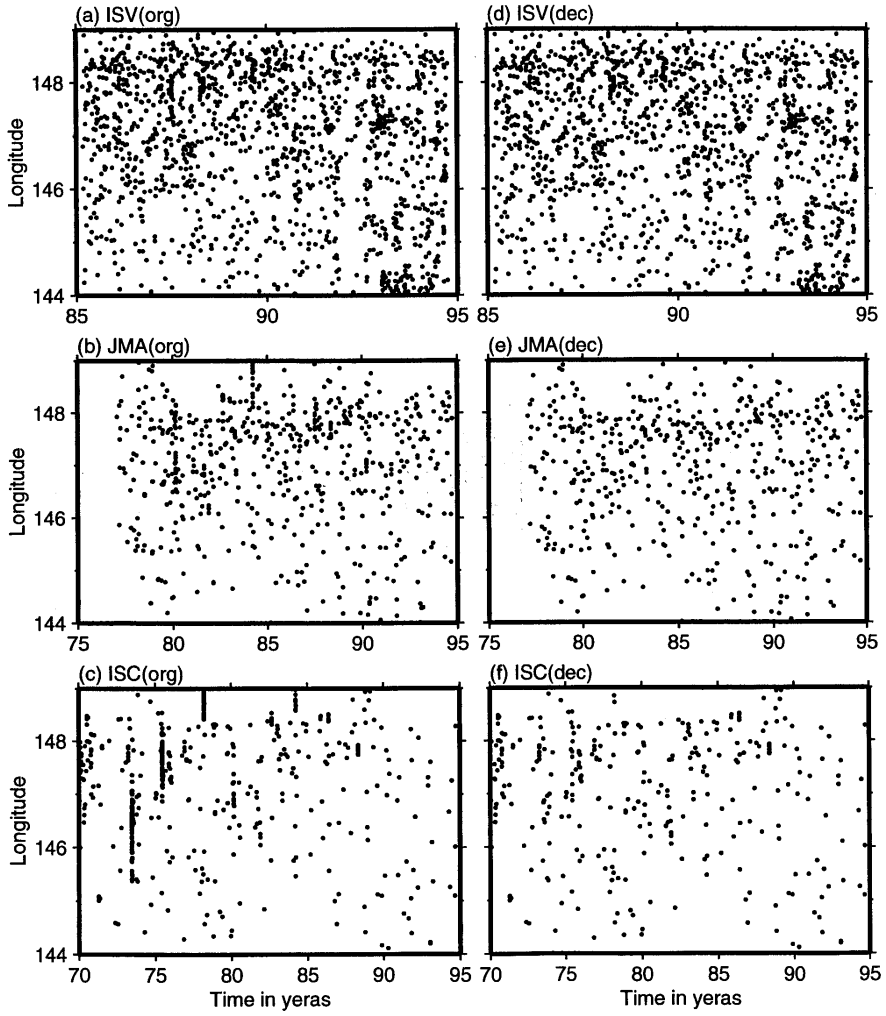

Figure 3
Space-time plots of earthquakes shown in Figure 2. (a)–(c) are original catalogs of ISV (1 March, 1985–3 October, 1994, $M \geq 3.0$), JMA (1 January, 1977–3 October, 1994, $M \geq 4.3$) and ISC (1 January, 1970–3 October, 1994, $M \geq 5.0$), respectively. (d)–(f) are declustered catalogs, excluding aftershocks and earthquake swarms from the original catalogs.

On space-time plots (Fig. 3a) the dependent events as aftershocks and swarms were carefully distinguished from background seismicity by hand; aftershocks were removed and outstanding swarms were substituted with the largest event in the sequence. This is a declustered catalog, including 1390 earthquakes, used in analysis (see Figs. 2d and 3d). There is scant difference: only 3% of the events were removed. As mentioned below, we have investigated that the process of declustering did not affect our results since this method is rather subjective.

2.2 JMA

JMA has its own seismic network in Japan and it has located hypocenters of earthquakes since 1926. The JMA hypocenter catalog has been generally used for research on seismicity in Japan. This catalog, however, has changed in quality because of the renewal of observation systems and the application of new techniques for data analysis (ICHIKAWA, 1987). In 1961 the manual calculation of the hypocenter was substituted by a computer system. JMA introduced a new travel timetable for the Kurile Islands region in 1978 (ICHIKAWA, 1978), and EMT equation in 1977 to estimate earthquake magnitudes (KANBAYASHI and ICHIKAWA, 1977; TAKEUCHI, 1983). Using the same method as applied to the ISV catalog to estimate magnitude completeness we obtained $M_c = 4.3$ for the JMA catalog, that is, earthquakes larger than $M = 4.3$ were uniformly reported in the target area and in the period between 1977 and 1994. Figures 2b and 3b show the epicenter map and a space-time plot including clustered events, respectively. After declustering (see Figs. 2e and 3e) the number of earthquakes was reduced from 946 to 491, with depths selected ranging from 0 to 150 km.

2.3 ISC

ISC publishes a monthly seismic bulletin, which is based on arrival times reported by regional seismic stations worldwide. ISC calculates hypocenters and magnitudes using these data. Thus the resulting catalog is independent of the ISV and the JMA catalogs (Figs. 2c and 3c). For the ISC catalog we estimated M_c as 5.0, using the same method as applied to the ISV and JMA catalogs. The declustered catalog includes 336 earthquakes larger than $M = 5.0$ located in the study area between 1 January, 1970 and 3 October, 1994 and depths selected from 0 to 150 km (Figs. 2f and 3f).

Figure 4 clearly shows the extent of time length and M_c of each catalog. The ISV catalog includes smaller events, therefore the number of declustered events is larger than that of the ISC catalog, though the time length is shorter. The JMA catalog contains features between those of the ISV and ISC catalogs.

3. Method

We have applied the ZMAP method (WIEMER and WYSS, 1994) to the three catalogs to image areas exhibiting a seismic quiescence. WIEMER and WYSS (1994) described details of the method. Therefore we only provide a brief summary in this paper. The study area was divided into grids spacing 0.1° in latitude and longitude (Table 2). A circle was drawn around each grid point and its radius was increased until it included a number N of earthquakes with magnitude larger than M_c. Such

circle defined the resolution circle for a given N. For ISV, JMA and ISC, the couples (M_c, N) were (3.0, 100), (4.3, 100) and (5.0, 50), respectively. In areas with higher seismicity the radius of the resolution circle is markedly smaller. For each circle we can plot the cumulative number of events vs. time. Only grid points with a resolution circle smaller than r km were selected, and their number is named N_{grid}. For ISV, JMA and ISC, the couples (r, N_{grid}) were (60 km, 470), (80 km, 414), and (80 km, 573), respectively. For each grid point, at any time t ($t_0 < t < t_e - T_w$), for a given time window T_w (Fig. 5), the Z-value is calculated by the equation,

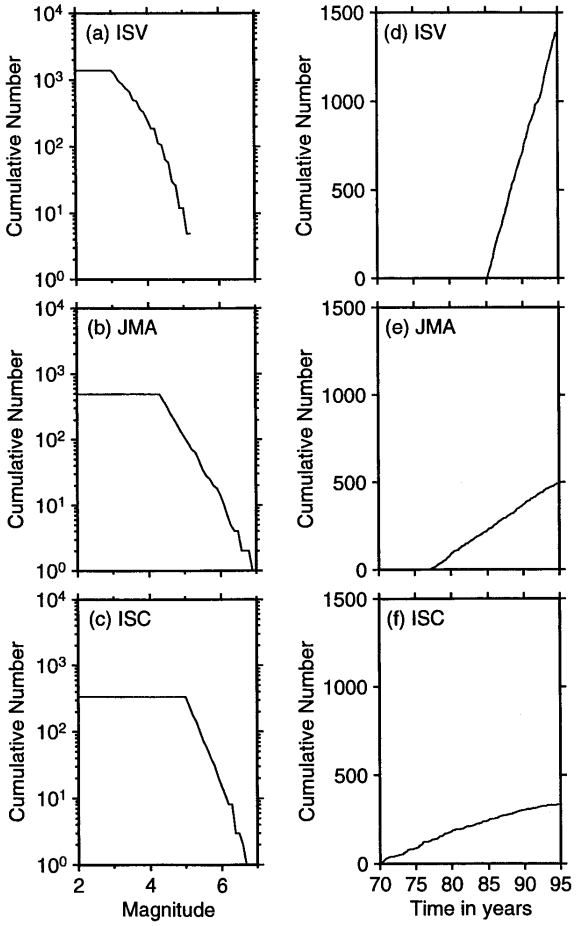

Figure 4
(a)–(c) are plots of the cumulative number of earthquakes shown in Figure 2 vs. magnitudes for the ISV, the JMA and the ISC catalogs, respectively. (d)–(f) are plots of the cumulative number vs. time for each catalog.

Table 2

Parameters used in the computer program ZMAP

Grid size	ISV $0.1° \times 0.1°$	JMA $0.1° \times 0.1°$	ISC $0.1° \times 0.1°$
Number of grids	470	414	573
Number of earthquakes in a circle	100	100	50
T_w (years)	5.0	5.0	5.0
Resolution radius (km)	60	80	80
Bin length (days)	12	22	30
Samples in a cumulative number plot	292	294	301

$$z(t) = \frac{(R_{\text{all}} - R_{wl})}{\sqrt{\frac{\sigma_{\text{all}}^2}{n_{\text{all}}} + \frac{\sigma_{wl}^2}{n_{wl}}}},$$

where R_{all} is the mean rate in the overall period including T_w (from t_0 to t_e), R_{wl} the mean rate in the considered time window (from t to $t + T_w$). σ_{all} and σ_{wl} are the standard deviations in these periods, and n_{all} and n_{wl} the number of samples. The Z-value, calculated for all times t between t_0 and $t_e - T_w$, by the equation is statistically appropriate for estimating seismicity rate change in a time window T_w in contrast with background seismicity.

When we detect the Z-value anomaly, we should also estimate how strong or how significant it is. For this purpose we used the alarm-cube method (WYSS and

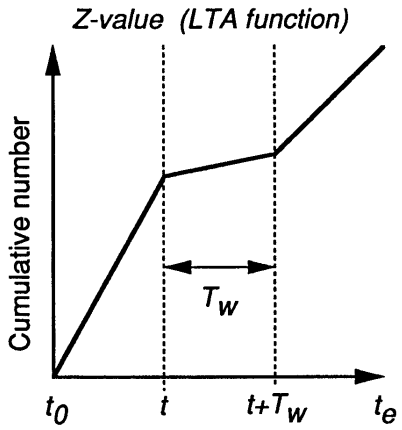

Figure 5

Schematic explanation of how to calculate Z-values. R_{all} is the mean rate in the overall period (from t_0 to t_e), R_{wl} the mean rate in the time window (from t to $t + T_w$), where t is the "current" time ($t_0 < t < t_e$) and T_w is the length of the time window in year. σ_{all} and σ_{wl} are the standard deviations in these periods, and n_{all} and n_{wl} the number of samples. The Z-value was calculated for all times t between t_0 and $t_e - T_w$ (see the text).

MARTIROSYAN, 1999): space-time search for anomalies. The space-time search illustrates in a space-time representation how often anomalies of the same kind as the one prior to the large event occurred in the study area. If similar anomalies appear frequently without any following large event, the reliability of the anomaly is judged very low. If the most significant seismic quiescence is followed by the largest event in the target area in all the time period, we can plausibly interpret the anomaly as a preparation process to that event.

4. Analysis

4.1 ZMAP

The Z-maps shown in Figure 6 present time slices for the ISV catalog every six month between 1986 and 1989.5 based on the declustered catalog. In Figures 7 and 8 the Z-maps for JMA and ISC catalogs were shown every year between 1982.5 and 1989.5. The time window, T_w, in which the mean rate is compared to the mean background rate, is 5 years. Though from all three catalogs a decrease of seismicity has been obviously detected in the target area, the shape of portions with the high Z-value anomaly (red areas) appears to be different. For ISV, there are two areas with the high Z-value (red areas) larger than $+4.0$. One is located west of 146°E on the maps from 1986.0 to 1987.5 (Anomaly ISV-1). Another one appears to be close to the initial point of the rupture of the 1994 Kurile mainshock on the maps from 1988.5 to 1989.0 (Anomaly ISV-2). Only one anomaly with high Z-value (a red area) was detected on JMA maps from 1987.5 to 1989.5 (Anomaly JMA-1). This anomaly is also located close to the initial point of the rupture. No anomaly corresponding to Anomaly ISV-1 was detected on the JMA maps. Anomaly ISV-2 is consistent with Anomaly JMA-1: both Anomaly ISV-2 and Anomaly JMA-1 started at a similar time and existed at a similar place. We believe that the common feature from the two catalogs is reliable and far from being due to man-made changes. Anomaly ISV-1 was probably a man-made change because no anomaly appeared west of 146°E on JMA maps. Therefore we concluded that Anamoly ISV-2 and Anomaly JMA-1 were the candidates of seismic quiescence associated with the 1994 Kurile mainshock. For ISC the pattern of the high Z-value anomaly (a red area) is rather different from that of ISV and JMA. The anomaly appears to surround the initial point of the rupture like a ring (Anomaly ISC-1). No change in

Figure 6
Time slices of Z-value distribution every six months between 1986 and 1989.5 using the ISV declustered catalog. The length of time window T_w is 5 years. Only grid points with a radius of resolution circle smaller than 60 km were selected. Their number is 470. The epicenter of the mainshock (+) and the aftershock area (a polygon bounded by a thin line) is indicated. Red color (positive Z-value) represents a decrease in seismicity rate.

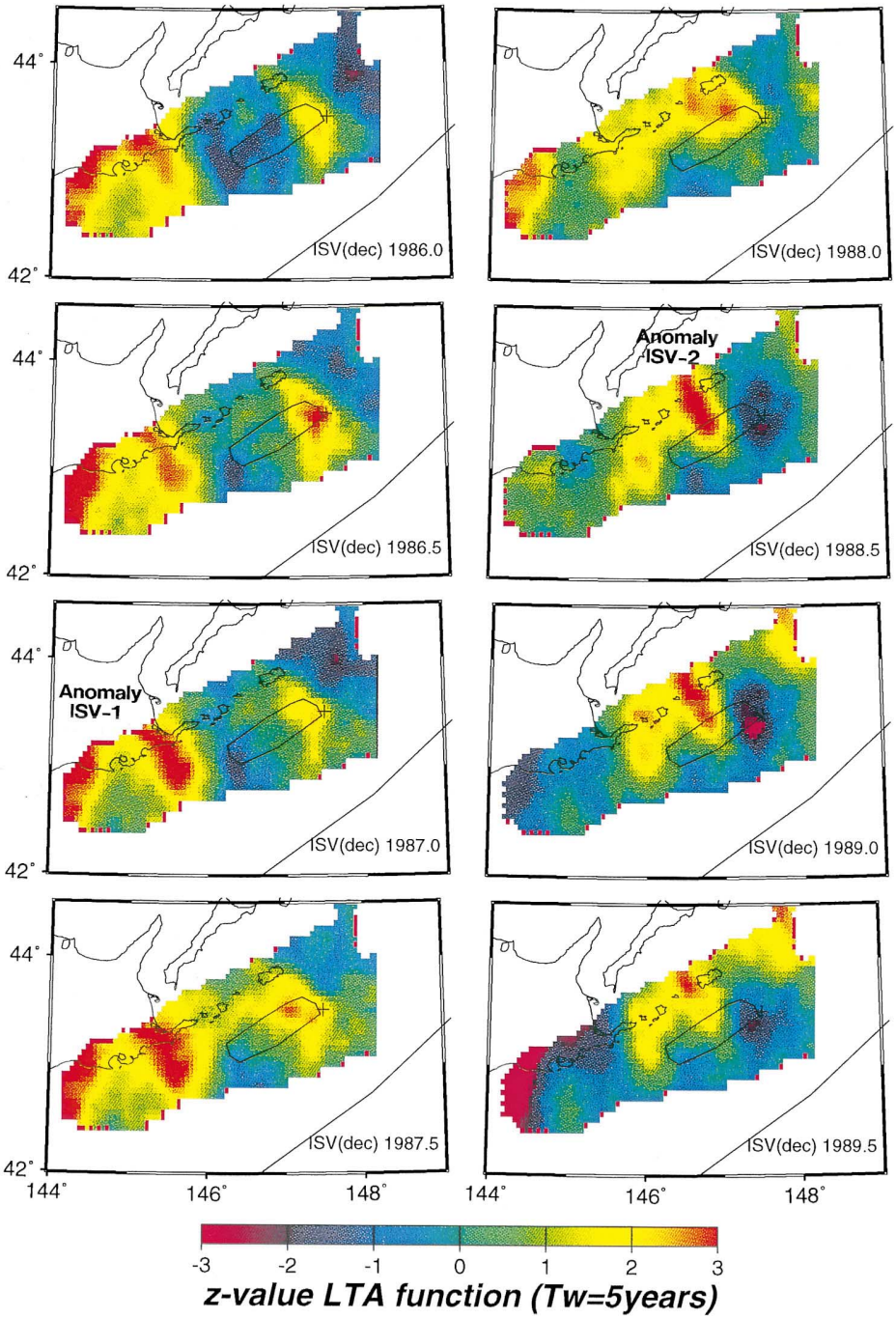
44°
42°
ISV(dec) 1986.0
ISV(dec) 1988.0
ISV(dec) 1986.5
Anomaly
ISV-2
ISV(dec) 1988.5
Anomaly
ISV-1
ISV(dec) 1987.0
ISV(dec) 1989.0
ISV(dec) 1987.5
ISV(dec) 1989.5
144°
146°
148°
-3
-2
-1
0
1
2
3
z-value LTA function (Tw=5years)

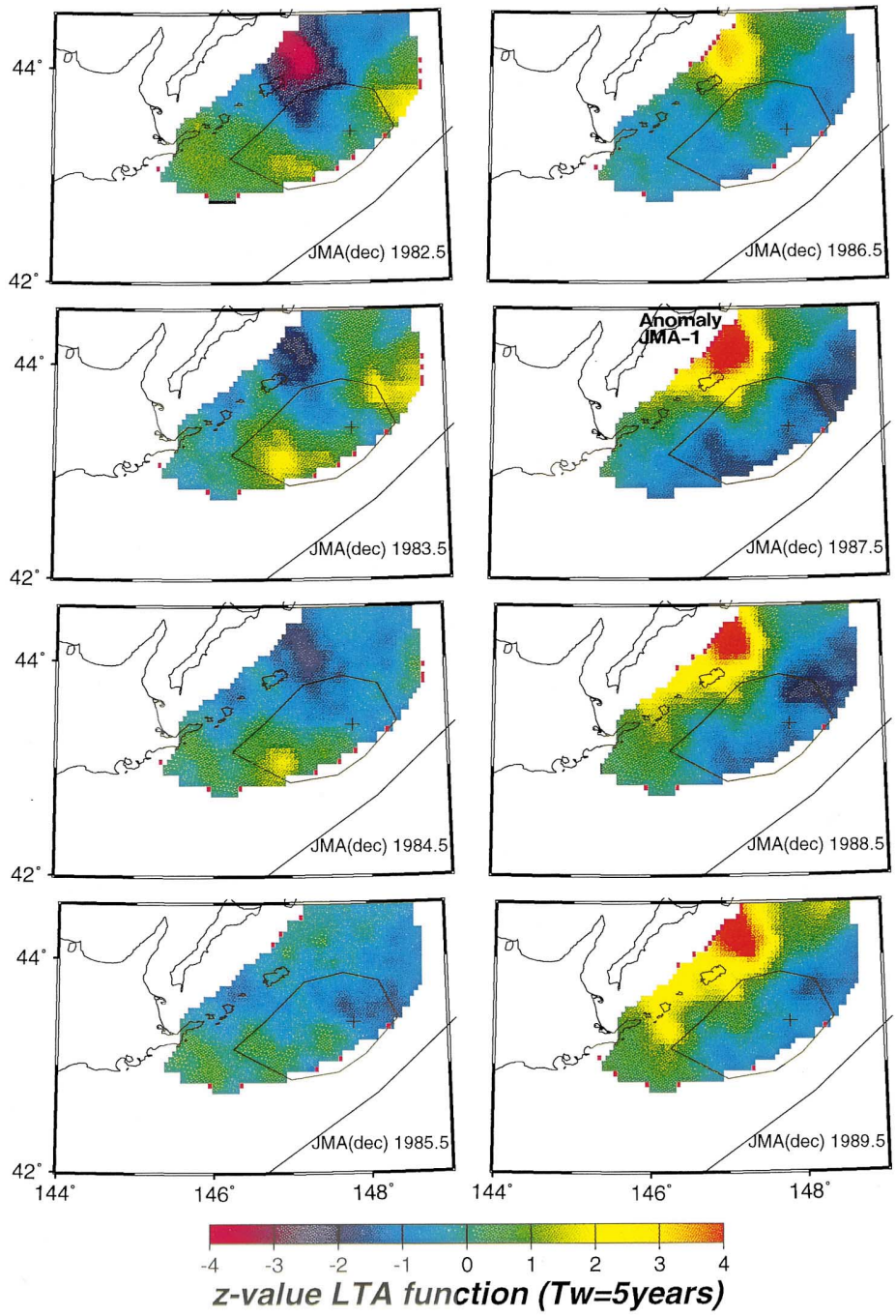
JMA(dec) 1982.5
JMA(dec) 1983.5
JMA(dec) 1984.5
JMA(dec) 1985.5
JMA(dec) 1986.5
Anomaly
JMA-1
JMA(dec) 1987.5
JMA(dec) 1988.5
JMA(dec) 1989.5
44°
42°
144°
146°
148°
-4 -3 -2 -1 0 1 2 3 4
z-value LTA function (Tw=5years)

seismicity rate was detected in a circle centered on the epicenter. This pattern is clearly delineated on the time slice at 1989.5: A red area indicating a decrease of seismicity extends from the aftershock area of the mainshock except for a circular area centered on the epicenter.

The cumulative curves in Figures 9a and 9b of the number of earthquakes as a function of time manifest seismicity rate changes at specific nodes in the cases of Anomaly ISV-2 and Anomaly JMA-1, respectively. These nodes were positioned randomly by the gridding process, however they were selected for presentation here because they were located in the anomalous areas mapped in Figures 6 and 7. The statistical functions, LTA, displayed in Figure 9 are the Z-values obtained by a comparison of the mean rate within a sliding time window and the long-term average, defined by overall seismicity, including the sliding time window, in the same volume. For ISV and JMA the Z-value peaked with $Z_{\max} = 4.0$ at 1988.8 and with $Z_{\max} = 5.2$ at 1989.3, respectively. Since a peak of Z-value reveals the time when the decrease of seismic rate starts, both clear anomalies were found to start at around 1989 and persist to the mainshock in 1994. For ISC we found a high Z anomaly with the shape of ring on the map at 1989.5 referring as Anomaly ISC-1. Therefore we selected earthquakes in the ring and made a cumulative number plot (Fig. 9c). A decrease of seismicity was clearly found in the ring and the Z-value took the maximum of $Z_{\max} = 6.8$ at 1989.5, which means that the decrease of seismicity started at 1989.5 and continued to the mainshock. On the other hand the rate was found to be rather constant in the circular area centered on the epicenter. Though the artificial shape of the ring made the statistical significance of this anomaly minor, the decrease in the ring should remain to be an outstanding candidate for a precursory quiescence.

We should be particularly attentive to the synchronization in time and space. All anomalies such as Anomaly ISV-2, Anomaly JMA-1 and Anomaly ISC-1 started around the year 1989 and lasted up until the mainshock in 1994, and they also existed very close to the focal area. However it is fact, from a statistical point of view, that the significance of quiescence was characterized by fairly low Z-values. Here $Z_{\max}$ values are typically of the order of three (one standard deviation). The largest $Z_{\max}$ value (6.8) was found for the anomaly of a particular shape brought to light with the ISC catalog.

Figure 7

Time slices of Z-values distribution every year between 1982.5 and 1989.5 using the JMA declustered catalog. The length of time window T_w is 5 years. Only grid points with a radius of resolution circle smaller than 80 km were selected. Their number is 414. The epicenter of the mainshock (+) and the aftershock area (a polygon bounded by a thin line) is indicated. Red color (positive Z-value) represents a decrease in seismicity rate.

4.2 Alarm Cube

The temporal and spatial correlation of the quiescence, mapped in Figures 6–8 and characterized in Figure 9, with the Kurile mainshock may have no significance, if similar quiescence anomalies occur frequently at locations in space and time where no mainshocks exist. Therefore we search the matrix of Z-values (generated by the LTA functions at all nodes) for high Z-values, which may approach, or exceed, the Z-values recorded by the anomaly before the Kurile earthquake. The display of the high Z-values that could be false alarms is made in the alarm-cubes (WIEMER, 1996; WYSS *et al.*, 1996; WYSS and MARTIROSYAN, 1999). In these 3-D figures (Fig. 10) horizontal axes are the spatial coordinates of the target area and the vertical axis is time. Alarms are defined as instances of Z-values larger than the selected alarm-level at any node and any time. Figure 10 illustrates that the results are stable, regardless of the seismic catalogs. The ISV's alarm cube includes two outstanding groups of anomalies: a group around the western end of the target area (Alarm ISV-1) and a group close to the epicenter of the mainshock (Alarm ISV-2). The JMA's alarm cube includes only one group of anomalies before and near the Kurile mainshock (Alarm JMA-1). Alarm ISV-1 obviously corresponds to Anomaly ISV-1 judged as a man-made change above. Alarm ISV-2 corresponds to Anomaly ISV-2 consistent with Anomaly JMA-1 and Alarm JMA-1. In the ISC's alarm cube, there were three groups of anomalies starting in 1984 (Alarm ISC-1), 1986 (Alarm ISC-2) and 1989 (Alarm ISC-3). Alarm ISC-1 and Alarm ISC-2 continued through 1989 and 1991, respectively. However no mainshock occurred. Alarm ISC-3 was ongoing through 1994 and the $M = 8.3$ Kurile mainshock occurred. Although all three alarm groups were located near the mainshock, the extent of the quiet area was very different. Alarm ISC-1 and Alarm ISC-2 were represented by only one or two bars in the alarm cube. Alarm ISC-3 appears as a cluster of bars close to the mainshock area. Since the area of Alarm ISC-3 was substantially larger than that of Alarm ISC-1 and ISC-2, Alarm ISC-3 can be considered more significant than Alarm ISC-1 and ISC-2. Moreover, only Alarm ISC-3 was consistent with Alarm ISV-2 and Alarm JMA-1 in time. Therefore we concluded that the alarm, which started around 1989 and existed close to the focal area, showed the only quiescence not depending on the seismic catalogs.

Figure 8

Time slices of Z-values distribution every year between 1982.5 and 1989.5 using the ISC declustered catalog. The length of time window T_w is 5 years. Only grid points with a radius of resolution circle smaller than 80 km were selected. Their number is 573. The epicenter of the mainshock (+) and the aftershock area (a polygon bounded by a thin line) is indicated. Red color (positive Z-value) represents a decrease in seismicity rate.

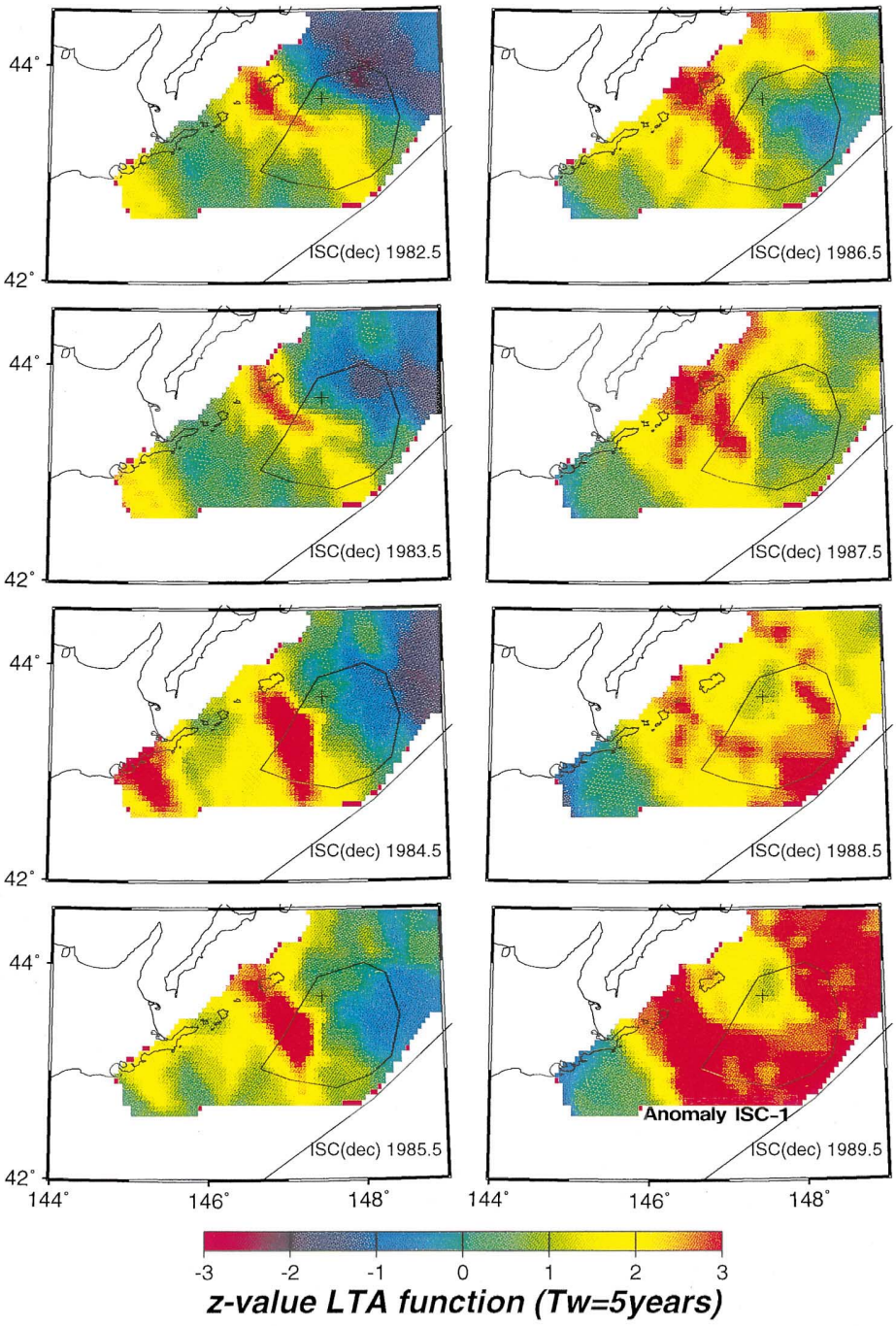
44°
42°
ISC(dec) 1982.5
ISC(dec) 1986.5
ISC(dec) 1983.5
ISC(dec) 1987.5
ISC(dec) 1984.5
ISC(dec) 1988.5
ISC(dec) 1985.5
Anomaly ISC-1
ISC(dec) 1989.5
144°
146°
148°
-3
-2
-1
0
1
2
3
z-value LTA function (Tw=5years)

4.3 Effect of Declustering Process

We have checked that the process of declustering did not affect our results. Figure 11 is a counterpart of Figure 9. Although Z_{max} for ISC in Figure 11c is smaller than that in Figure 9c, we were also able to detect that the seismic

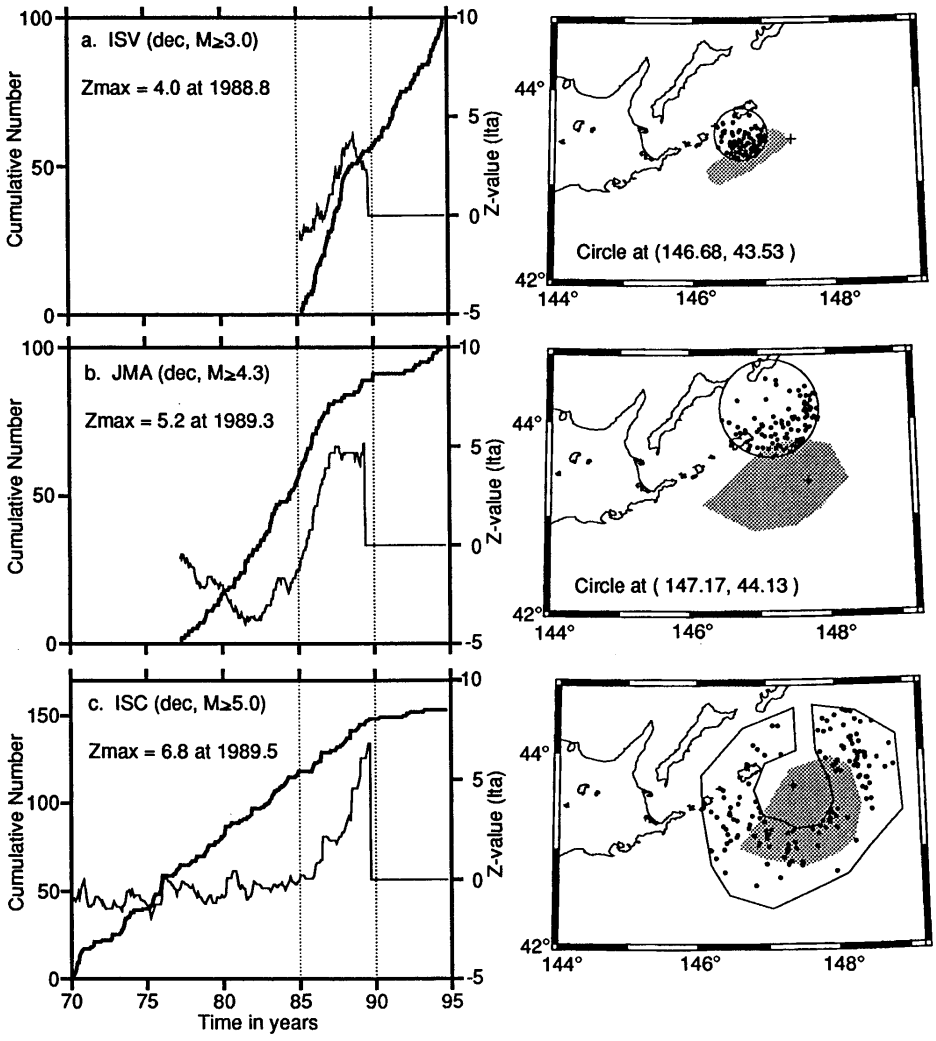

Figure 9
Cumulative number plots for anomalous areas detected in Figures 6–8. (a) Anomaly ISV-2, (b) Anomaly JMA-1 and (c) Anomaly ISC-1 (see in the text). Bold and thin lines in the cumulative number plots show cumulative numbers and Z-values as a function of time, respectively. Maps at the right of each cumulative number plots show the anomalous areas and aftershock areas (hatched portions) and the epicenters of the mainshock (+).

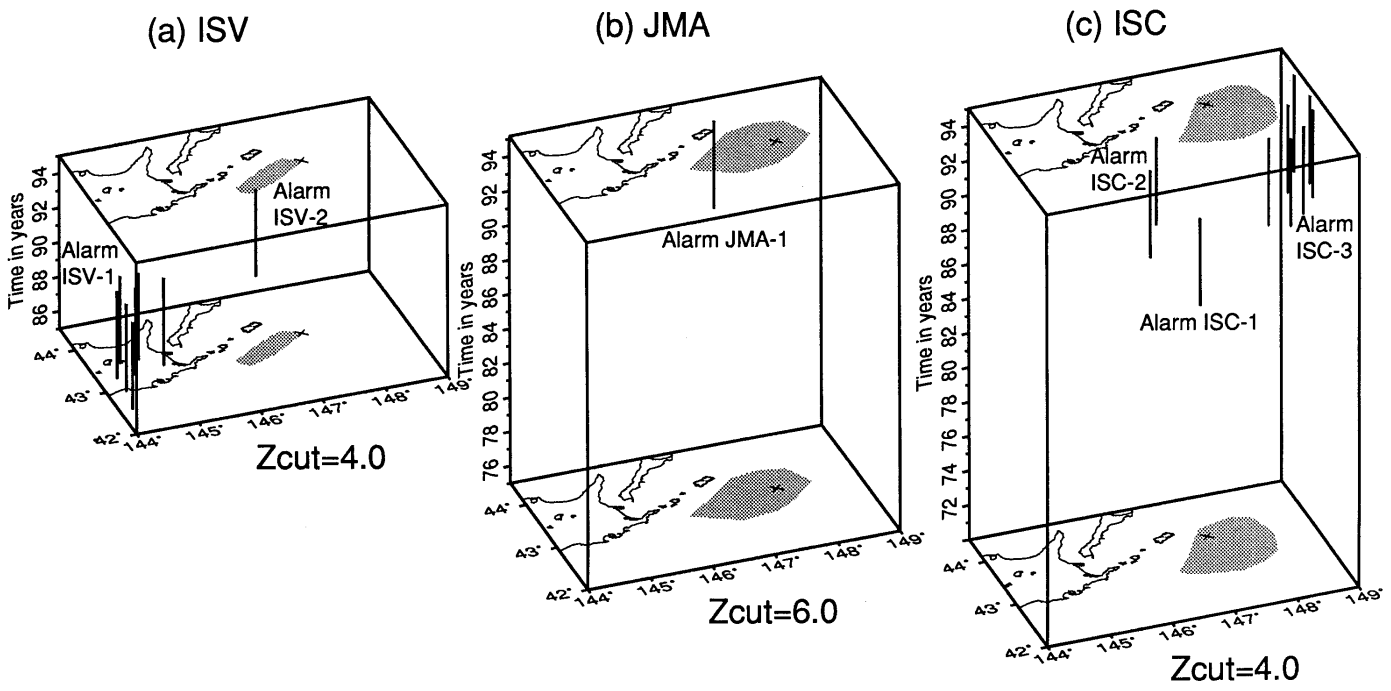

Figure 10
Alarm cubes for (a) ISV, (b) JMA and (c) ISC. Vertical bold lines with a time length of 5 years indicate alarms with Z-values larger than Z_{cut}. Hatched areas and (+) s show the aftershock area and the epicenter of the mainshock, respectively.

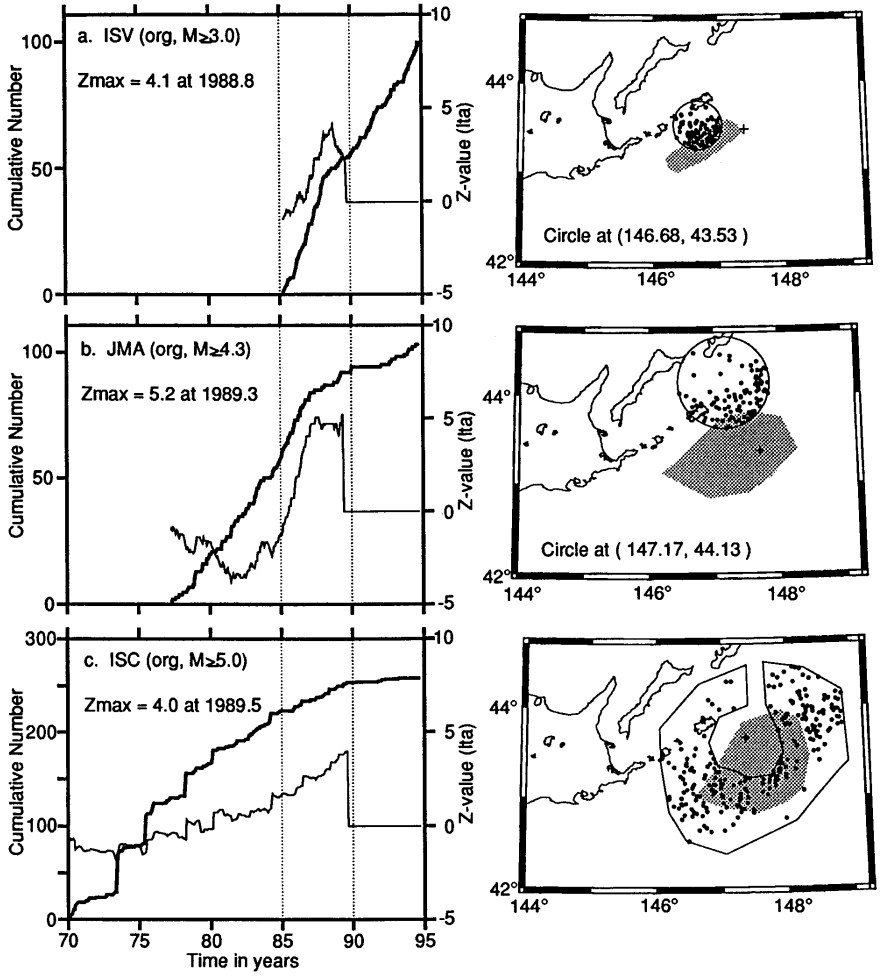

Figure 11
Same plots as Figure 9 except for the use of the original (clustered) catalogs of (a) ISV, (b) JMA and (c) ISC.

quiescence started around 1989 and was located near the aftershock area of the mainshock.

4.4 Magnitude Signatures

Since an apparent seismic quiescence is often caused by man-made changes, we should carefully examine the quiescences found. In particular, magnitude shift and stretch critically affect the results (WIEMER and WYSS, 1994). Figure 12 shows

magnitude signatures for ISV comparing two time windows: before and after the start of quiescence. In these plots we used all earthquakes regardless of magnitude. In the quiescence area with high Z-value, b-values were similar in the two time windows (Fig. 12d) and the number of earthquakes decreased in all magnitude bands between $M = 1$ and 4. Therefore, we concluded that this quiescence was not

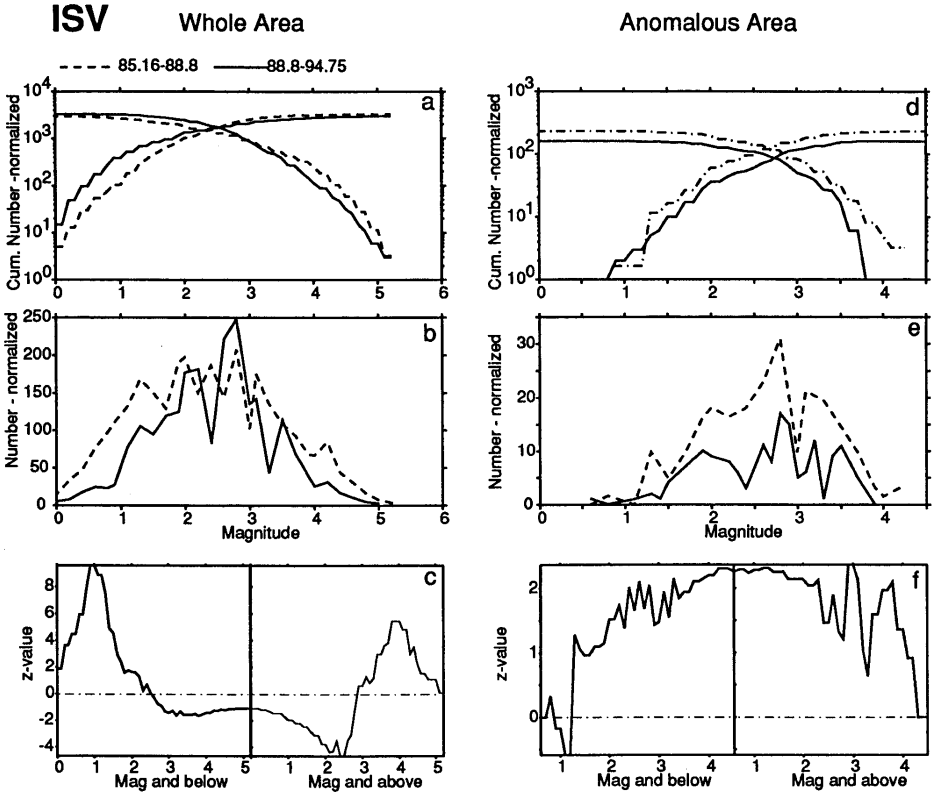

Figure 12

Magnitude signatures for the declustered ISV catalog. All earthquakes regardless of magnitude are used. Broken and bold lines indicate the normal period (1985.16–1988.8) and the quiescence period (1988.8–1994.75), respectivley. (a) and (d) are plots of magnitude vs. the cumulative number for the entire target area and the high-Z (Anomaly ISV-2) area, respectively. (b) and (e) are plots of magnitude vs. frequency for the entire target area and the high-Z (Anomaly ISV-2) area, respectively. (c) and (f) are plots of magnitude vs. Z-value for the entire target area and the high-Z (Anomaly ISV-2) area, respectively. The label "Mag and below" on horizontal axes in (c) and (f) means that Z-values are calculated for earthquakes with a magnitude equal to or less than the values indicated on the axis scale. The label "normalized" in (a), (b), (d) and (e) means that the number of earthquakes is normalized in time because two time periods comparing each other have a different time length. For instance, assume that the length of Period 1 is one year and that of Period 2 is two years. If the seismicity rate is constant, we will observe two times earthquakes in Period 2 more than in Period 1. Thus the number of earthquakes in Period 2 is divided by two in the normalization process.

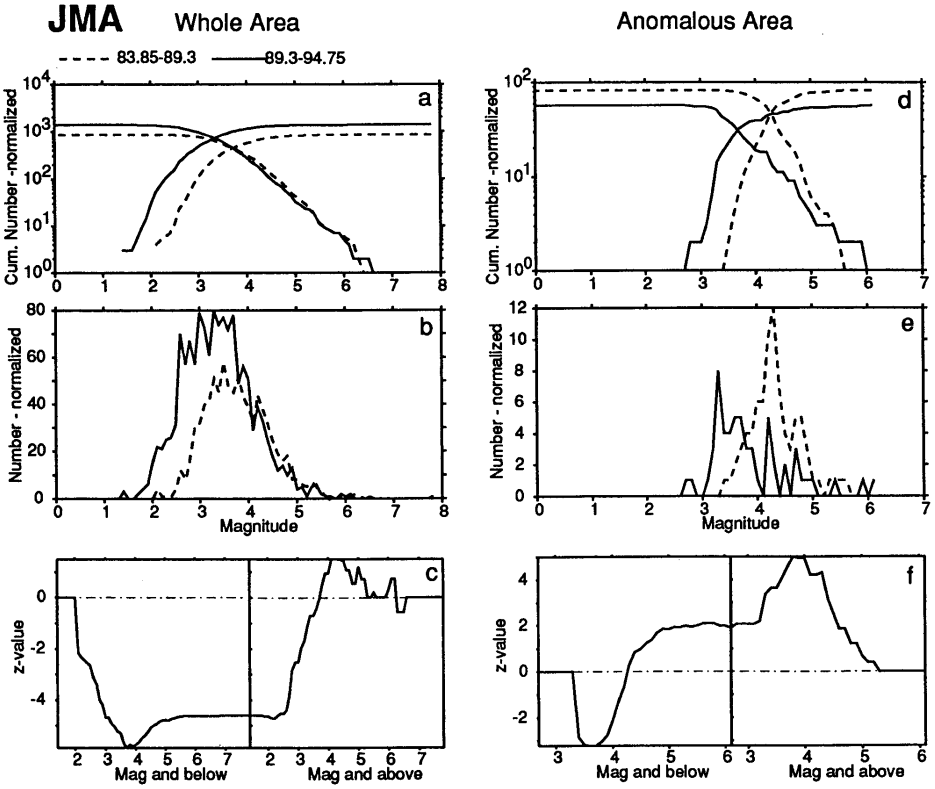

Figure 13
Magnitude signatures for the declustered JMA catalog. All earthquakes regardless of magnitude are used. Broken and bold lines indicate the normal period (1983.85–1989.3) and the quiescence period (1989.3–1994.75), respectively. (a)–(c) and (d)–(f) are plots for the entire target area and the high-Z (Anomaly JMA-1) area, respectively. The meaning of each plot is the same as in Figure 12.

an artifact caused by man-made changes. Figure 13 shows magnitude signatures for JMA comparing two time windows: before and after the start of quiescence. In the anomalous area with high Z-value, b-values in the magnitude-frequency plot (Fig. 13d) decreased from 0.91 to 0.77. The decrease of earthquakes larger than $M =$ 3.5–4.0 and the increase of earthquakes smaller than $M = 3.5$–4.0 induced this change in b-value. It seems that a systematic shift in magnitude-frequency distribution occurred in 1989. In the entire target area, the detection was drastically advanced in earthquakes smaller than $M = 4$ (Fig. 13b). The b-values and the number of located earthquakes larger than $M = 4$, however, did not change (Figs. 13a and 13b), that means that there was no significant magnitude shift and stretch

in the entire target area in 1989. Thus the change in b-value occurred only in the anomalous area. Therefore, we concluded that the decrease of earthquakes larger than $M = 4$ was probably not caused by any man-made change. Figure 14 displays magnitude signatures for ISC in the ring area which has the unusual high Z-value. Three time windows were selected to compare the seismicity: before the quiescence (1984.25–1989.5, Period 1), the time between the starting point of the quiescence and the mainshock (1989.5–1994.75, Period 2), and after the mainshock (1994.75–1995.1, Period 3). Note that earthquakes in Period 3 were not included in the data

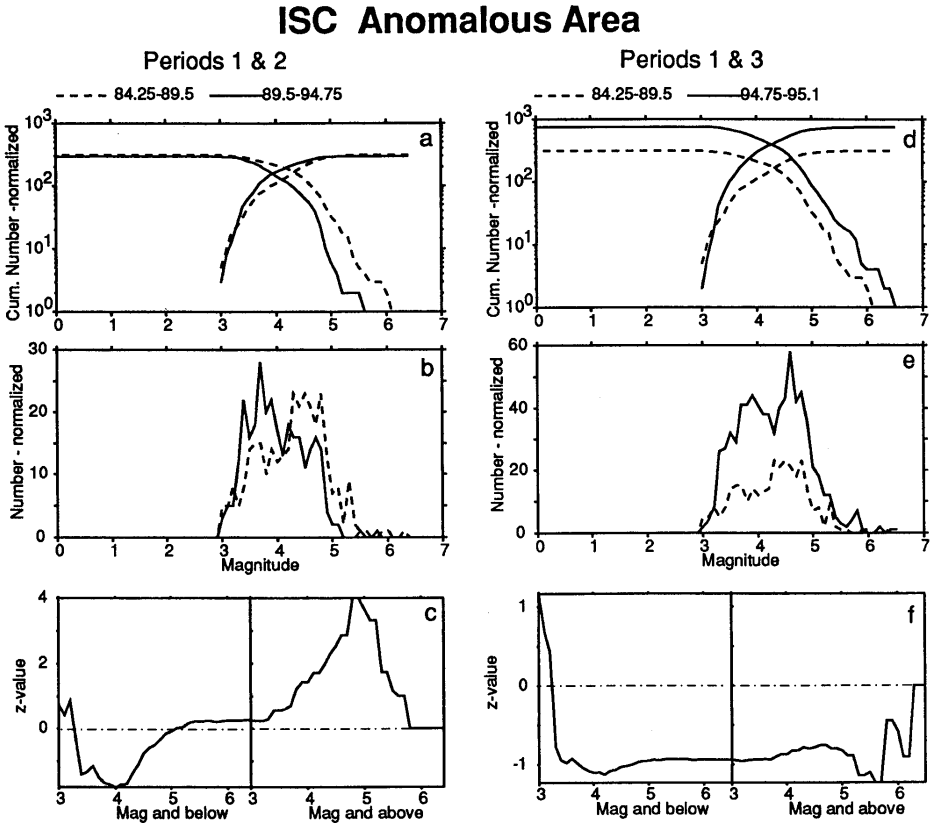

Figure 14
Magnitude signatures for the declustered ISC catalog. All earthquakes regardless of magnitude are used in the Anomaly area ISC-1. Three time windows were selected to compare the seismicity: before the quiescence (1984.25–1989.5, Period 1), the time between the starting point of the quiescence and the mainshock (1989.5–1994.75, Period 2), and after the mainshock (1994.75–1995.1, Period 3). In (a)–(c) Period 1 (broken lines) is compared with Period 2 (solid lines). In (d)–(f) Period 1 (broken lines) is compared with Period 3 (solid lines). The meaning of each plot is the same as in Figure 12.

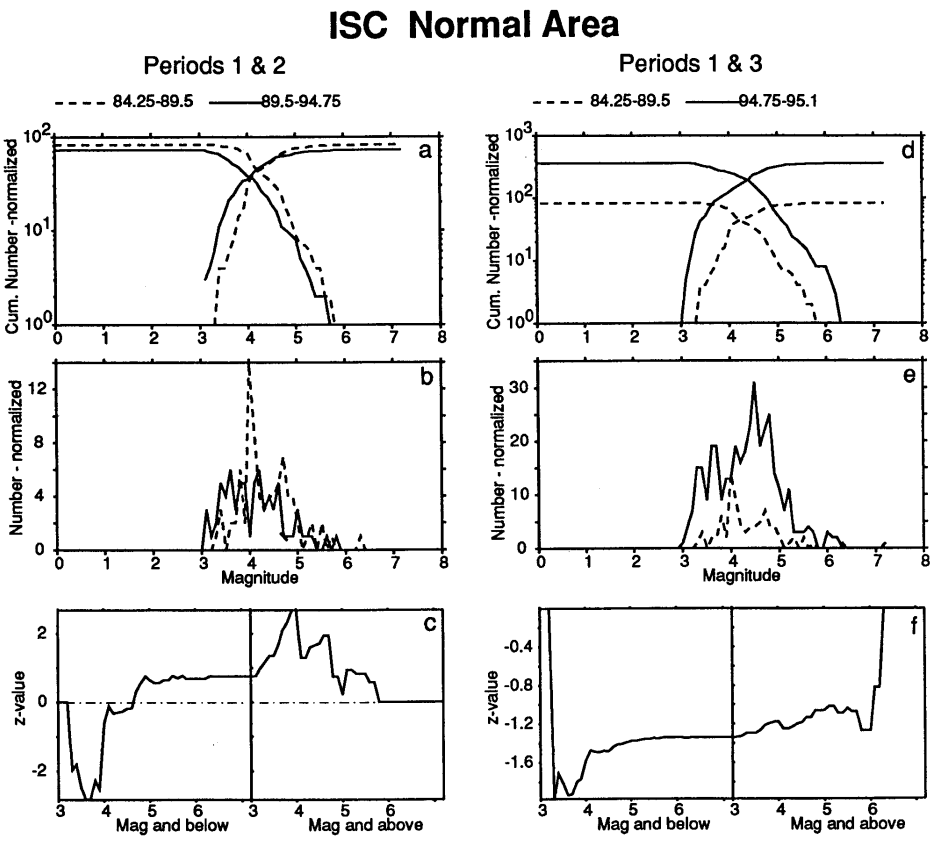

Figure 15
Magnitude signatures for the declustered ISC catalog. All earthquakes regardless of magnitude are used in the circular area centered on the epicenter of the mainshock, which did not exhibit seismic quiescence. The time is divided into three periods as mentioned in Figure 14. The meaning of each plot is the same as in Figure 12.

set to make Z-maps, but added only for the magnitude signature. In the ring area the decrease of earthquakes larger than $M = 4$ is outstanding when comparing Periods 1 and 2. In Period 2 events smaller than $M = 4$ were more detected in Period 1. Thus a magnitude shift appeared to occur in Period 2, caused by a man-made change, and a seismic quiescence might be found for earthquakes larger than $M = 4$. However, this is not plausible. Comparing Periods 1 and 3, such type of magnitude shift was not found. The b-values were the same (Fig. 14d) and earthquakes larger than $M = 4$ were similarly detected in Period 1 and Period 3. The shape of magnitude-number plots in Figure 14e in Period 1 is similar to that in Period 3. Figure 15 presents magnitude signatures for the circular area centered on the epicenter of the mainshock, which did not exhibit the seismic quiescence.

There was no significant decrease of seismicity in Period 2 compared with Period 1, and no significant change in b-values (Fig. 15a) and a pattern of frequency-magnitude plots (Fig. 15b). Comparing Period 1 with Period 3 we recognized neither a clear magnitude shift nor a magnitude stretch (Figs. 15d–f). Therefore we have concluded that the quiescence in the ring area in Period 2 was not caused by any man-made change but rather change in geophysical conditions in and around the focal area of the 1994 Kurile mainshock.

4.5 Comparing JMA and ISC Catalogs

The seismic quiescence associated with Anomaly ISC-1 and Alarm ISC-3 also has been detected using the JMA catalog. In Figure 16 we plotted the cumulative number vs. time using the JMA catalog for earthquakes larger than $M = 4.8$ in the ring area shown in Figure 9c. The Z-value clearly peaked at 1989.3, which is the same pattern as that pictured in Figure 9c. We should next discuss whether the JMA catalog is independent of the ISC catalog. JMA certainly provides arrival times of seismic waves with ISC and the data are used to calculate hypocenters. However, in the case of earthquakes with $M = 5.0$ and larger, the data from JMA are only a part of reports from seismic stations worldwide. For instance, ISC used 141 seismic stations including 35 stations of JMA to locate the $M = 5.0$ earthquake in the study area on 19 November, 1991. Therefore, we assumed that the ISC catalog is independent of the JMA catalog for earthquakes with $M = 5.0$ and larger. Thus the seismic quiescence in the ring area has been confirmed by two independent seismic catalogs.

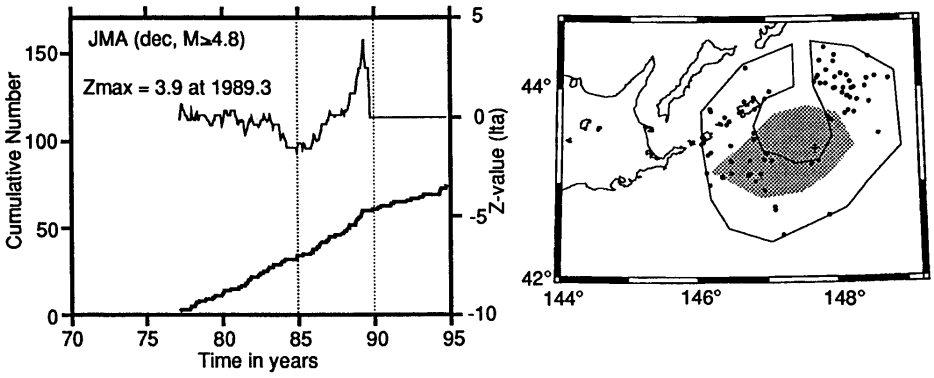

Figure 16
Cumulative number plot for earthquakes larger than $M = 4.8$ in the area of Anomaly ISC-1 using the JMA catalog.

Table 3

Parameters of precursory quiescence to the $M_w = 8.3$ Kurile 1994 earthquake

Catalog	Sample size N	Window length T_w (years)	Relative significance $Z_{\max}$	Start t_Q (date)	Duration T_Q (years)	Radius 75% r (km)
ISV	100	5	4.0	88.8	6.0	24
JMA	100	5	5.2	89.3	5.5	53
ISC	153	5	6.8	89.5	5.3	–

4.6 Spatial Extent of the Quiescence Anomaly

We define the spatial extent of the quiescence anomaly by the area in which a 75% rate decrease occurred for the ISV and JMA catalogs. This criterion (WIEMER and WYSS, 1994) is arbitrary. In this paper, we define the area of 75% rate decrease employing the same method as WYSS and MARTIROSYAN (1999): we increase the radius of a circle, centered at the coordinates of the largest Z-value, until the rate decrease is 75%. If more than one node has the same $Z_{\max}$, we select the one that leads to the larger anomaly volume. As mentioned by WYSS and MARTIROSYAN (1999), this method is advantageous in that it is clearly defined and can be repeated. However, it is disadvantageous in that it does not map the quiescence volume optimally because we should accept a circle as the anomaly shape, though the shape is not usually defined by a circle. Depending on the catalogs chosen, the radii of the 75% circular quiescence anomaly before the Kurile earthquake are 24 km for ISV and 53 km for JMA (Table 3). Since the ISC catalog includes a number of earthquakes too small to apply this method, we did not estimate a radius for ISC. However, the quiescence area of ISC is evidently larger than that of ISV and JMA. The area of a seismic quiescence possibly changes as a function of the magnitude band.

4.7 Duration of the Quiescence Anomaly

We define the duration of the Kurile quiescence, T_Q, as the time from the largest report of Z-value for the LTA(t) function, t_Q, to the mainshock. Onset time and duration vary somewhat as a function of the catalog chosen (Table 3). The duration time ranges from 5.3 to 6.0 years and the quiescence starts between 1988.8 and 1989.5.

5. Discussion and Conclusions

The three catalogs used in this study have differing quality from the standpoint of homogeneous reporting in the area of Figure 2. Though the ISC catalog provides

long-term data, earthquakes smaller than $M = 5.0$ are not reported homogeneously. Though the ISV catalog includes smaller events down to $M = 3.0$, the period of observation is shorter. Regardless of these differences we have found that results obtained from all three catalogs are mostly consistent with each other: the seismic activity started to decrease 5.3–6.0 years before the 1994 Kurile mainshock near the ruptured area. The seismic quiescence detected in this study is unusually significant and not caused by man-made change.

Nonetheless there are problems and limitations for the analysis in this study: (1) The geographical extension of the area considered in this paper (5° longitude by 2.5° latitude) appears insufficiently large in comparison with the presumable extension of the source area of an earthquake of magnitude $M_w = 8.3$. Moreover, the actual size of the area where the density of data was high enough for the analysis to be carried out, is less than 50% of the total. Therefore, strictly speaking, it is not possible to compare the seismicity pattern in the area affected by the source preparation process with other areas distant from the source. This circumstance is particularly evident with the ISC data, where the quiescence occupies most of the studied area. In this case, the significance of the anomaly as a precursor, estimated by the ration of the alarm volume and the total time-space volume, is not very good. (2) The temporal extension of the ISV catalog (9.6 years) appears rather short in comparison with the time length of he observed anomaly (6.0 years). In this circumstance it is hard to recognize the quiescence as an anomalous behavior if neither the JMA nor ISC catalog manifested the quiescence. (3) There is the different size and shape of the aftershock area among the three catalogs. Though the aftershock areas in JMA and ISC are approximate, the area of ISV appears to be smaller than JMA and ISC. KATSUMATA *et al.* (1995) found that some aftershocks were induced after the mainshock (Type 2 activity) and the largest aftershock and its aftershocks were located at the eastern end of the seismic fault ruptured by the mainshock (Type 3 activity). In this paper we plotted an area that excluded Types 2 and 3 activities on ISV maps. The aftershock areas on JMA and ISC maps include all aftershocks within one month after the mainshock because we hardly distinguished the detailed distributions such as Types 2 and 3. (4) There exists the different size and shape of the quiescence area among the three catalogs. Our hypothesis holds that as a magnitude band shifts larger, a quiescence area becomes wider. Another hypothesis maintains that a quiescence area should have constant size, shape and location regardless of magnitude band. If this is correct, the differences among the three catalogs reduce the reliability of the comparison. However both hypotheses should be tested and proved by future studies.

TAKANAMI *et al.* (1996) have found that a seismic quiescence started three years before the Kurile mainshock in the vicinity of the ruptured area. They used only the ISV catalog and earthquakes larger than $M = 3.5$ due to the incompleteness of the catalog. Our results are mostly consistent with TAKANAMI *et al.* (1996). However,

TAKANAMI *et al.* (1996) did not mention whether or not the quiescence they found was a man-made change.

Previous works on a seismic quiescence generally used only one seismic catalog and did not compare two or three independent catalogs. In these cases we can hardly estimate whether the quiescence is a fact or a man-made change. For instance TAYLOR *et al.* (1991) used only the ISV catalog to find a seismic quiescence before the $M_{\mathrm{JMA}} = 7.1$ Urakawa-Oki earthquake, WIEMER and WYSS (1994) used only a seismic catalog of the California Institute of Technology for the $M = 7.5$ Landers earthquake, WYSS and BURFORD (1985) used only the central California seismograph network for the $M_L = 4.6$ San Andreas earthquake, KISSLINGER (1988) utilized only the central Aleutians (Adak) seismic network for the $M_w = 8.0$ Andreanof Islands earthquake and WYSS *et al.* (1981) used only the Hawaiian Volcano Observatory for the $M = 7.2$ Kalapana earthquake. In this paper we have analyzed three independent seismic catalogs, including ISV, JMA and ISC, and found that all three catalogs clearly manifested the seismic quiescences prior to the $M_w = 8.3$ Kurile earthquake. This fact strongly suggests that the seismic quiescences detected in this paper are more reliable than those in previous studies.

KATSUMATA and KASAHARA (1999) have reported that the eastern Hokkaido and the southern Kurile Islands around the focal area exhibited steep subsidences synchronized with the seismic quiescence detected in this study. Earthquake instability models predict that a preseismic stable sliding the time scale occurs several years before an unstable (earthquake) faulting, and may affect the background seismicity (SHIBAZAKI and MATSU'URA, 1992; DIETERICH, 1992; KATO *et al.*, 1997). KATSUMATA and KASAHARA (1999) proposed the preseismic stable sliding on the same fault as the mainshock to model the subsidences and the seismic quiescence.

Moreover, ISV reported to the Coordinating Committee for Earthquake Prediction in August 1994 that six strain meters in the eastern Hokkaido had displayed clear changes since 1991 (HOKKAIDO UNIVERSITY, 1994). At that time they were not able to sound the alarm because of lack of data: they had definitely recognized neither the seismic quiescence detected in this study nor the crustal deformation anomaly pointed out by KATSUMATA and KASAHARA (1999). If they had known all these anomalies and had suitably accomplished a computer simulation using an earthquake instability model, they might have forecasted that a sizeable earthquake would have occurred in the southern Kurile Islands within several years.

In conclusion, the Kurile earthquake in 1994 provided us with an important lesson: simultaneous detection of seismic quiescence and crustal deformation anomaly are keys to the success of intermediate-term earthquake prediction. Moreover, if we use two or three independent catalogs, we provably detect a seismic quiescence before a mainshock, even though the catalogs are not perfectly complete. Therefore we should more carefully monitor seismicity and crustal deforma-

tion to detect intermediate-term anomalies prior to a great earthquake in the near future.

Acknowledgements

We thank V.G. Kossobokov at Intl. Inst. Earthquake PT&MG, T. Takanami, Y. Motoya and N. Wada at ISV, M. Wyss at University of Alaska, Fairbanks and two anonymous referees for helpful comments. S. Wiemer provided us with the program ZMAP.

REFERENCES

DIETERICH, J. H. (1992), *Earthquake Nucleation on Faults with Rate- and State-dependent Strength*, Tectonophysics *211*, 115–134.

FURUKAWA, N. (1995), *Quick Aftershock Relocation of the 1994 Shikotan Earthquake and its Fault Planes*, Geophys. Res. Lett. *22*, 3159–3162.

HABERMANN, R. E., *The Quantitative Recognition and Evaluation of Seismic Quiescence: Applications to Earthquake Prediction and Subduction Zone Tectonics*, Ph.D. Thesis (University of Colorado, Boulder 1981a).

HABERMANN, R. E., *Precursory seismicity patterns: Stalking the mature seismic gap*. In *Earthquake Prediction* (eds. D. W. Simpson and P. G. Richards), Maurice Ewing Series (Amer. Geophys. Union 4 1981b) pp. 29–42.

HABERMANN, R. E. (1987), *Man-made Change of Seismicity Rates*, Bull. Seismol. Soc. Am. *77*, 141–159.

HABERMANN, R. E. (1991), *Seismicity Rate Variations and Systematic Changes in Magnitudes in Teleseismic Catalogs*, Tectonophysics *193*, 277–289.

HABERMANN R. E., and WYSS, M. (1984), *Seismic Quiescence and Earthquake Prediction on the Calaveras Fault*, *California*, Abstract, EOS *65*, 988.

HIRATA, N., and MATSU'URA, M. (1987), *Maximum-likelihood Estimation of Hypocenter with Origin Time Eliminated Using Nonlinear Inversion Technique*, Phys. Earth. Planet. Int. *47*, 50–61.

HOKKAIDO UNIVERSITY (1994), *Continuous Observation of Crustal Deformation in Hokkaido Region—Strain Accumulation of 9 Stations for the Period from May*, *1987 to November*, *1992*, Report of the Coordinating Committee for Earthquake Prediction *52*, 45–55 (in Japanese).

ICHIKAWA, M. (1978), *A New Subroutine Program for Determination of Earthquake Parameters and Local Travel-time Tables for Events near the Southern Kurile Trench* (in Japanese with English abstract), Quarterly J. Seismology *43*, 11–19.

ICHIKAWA, Y. (1987), *Change of JMA Hypocenter Data and Some Problems*, Quarterly J. Seismology *51*, 47–56.

KANBAYASHI, Y., and ICHIKAWA, M. (1977), *A Method for Determining Magnitude of Shallow Earthquakes Occurring in and near Japan*, Quarterly J. Seismology *41*, 57–61.

KATO, N., OHTAKE, M., and HIRASAWA, T. (1997), *Possible Mechanism of Precursory Seismic Quiescence: Regional Relaxation due to Preseismic Sliding*, Pure appl. geophys. *150*, 249–267.

KATSUMATA, K., ICHIYANAGI, M., MIWA, M., KASAHARA, M., and MIYAMACHI, H. (1995), *Aftershock Distribution of the October 4, 1994 M_w 8.3 Kurile Islands Earthquake Determined by a Local Seismic Network in Hokkaido*, *Japan*, Geophys. Res. Lett. *22*, 1321–1324.

KATSUMATA, K., and KASAHARA, M. (1999), *Precursors to the 1994 Kurile Earthquake ($M_w = 8.3$)*, in preparation.

KIKUCHI, M., and KANAMORI, H. (1995), *The Shikotan Earthquake of October 4, 1994: Lithospheric Earthquake*, Geophys. Res. Lett. *22*, 1025–1028.

KISSLINGER, C. (1988), *Prediction of the May 7, 1986 Andreanof Islands Earthquake*, Bull. Seismol. Soc. Am. *78*, 218–229.

MCNALLY, K., *Plate subduction and prediction of earthquakes along the middle America trench*. In *Earthquake Prediction* (eds. D. W. Simpson and P. G. Richards), Maurice Ewing Series (Am. Geophys. Union 4 1981) pp. 63–72.

MOGI, K. (1969), *Some Features of Recent Seismic Activity in and near Japan (2), Activity before and after Great Earthquakes*, Bull. Earthq. Res. Inst., Univ. Tokyo *47*, 395–417.

OHTAKE, M., MATSUMOTO, T., and LATHAM, G. V. (1977), *Seismic Gap near Oaxaca, Southern Mexico as a Probable Precursor to a Large Earthquake*, Pure appl. geophys. *115*, 375–385.

OZAWA, S. (1996), *Geodetic Inversion for the Fault Model of the 1994 Shikotan Earthquake*, Geophys. Res. Lett. *23*, 2009–2012.

SHIBAZAKI, B., and MATSU'URA, M. (1992), *Spontaneous Process for Nucleation, Dynamic Propagation, and Stop of Earthquake Rupture*, Geophys. Res. Lett. *19*, 1189–1192.

TAKANAMI, T., SACKS, I. S., SNOKE, A., MOTOYA, Y., and ICHIYANAGI, M. (1996), *Seismic Quiescence before the Hokkaido-Toho-Oki Earthquake of October 4, 1994*, J. Phys. Earth *44*, 193–203.

TAKEUCHI, H. (1983), *Magnitude Determination of Small Shallow Earthquakes with JMA Electromagnetic Seismograph Model 76*, Quarterly J. Seismology *47*, 112–116.

TANIOKA, Y., RUFF, L., and SATAKE, K. (1995), *The Great Kurile Earthquake of October 4, 1994 Tore the Slab*, Geophys. Res. Lett. *22*, 1661–1664.

TAYLOR, D. W. A., SNOKE, J. A., SACKS, I. S., and TAKANAMI, T. (1991), *Seismic Quiescence before the Urakawa-Oki Earthquake*, Bull. Seismol. Soc. Am. *81*, 1255–1271.

TSUJI, H., HATANAKA, Y., SAGIYA, T., and HASHIMOTO, M. (1995), *Coseismic Crustal Deformation from the 1994 Hokkaido-Toho-Oki Earthquake Monitored by a Nationwide Continuous GPS Array in Japan*, Geophys. Res. Lett. *22*, 1669–1672.

URABE, T., and TSUKADA, S. (1992), *WIN—A Workstation Program for Processing Waveform Data from Microearthquake Networks* (abstract in Japanese), Programme and Abstracts, Seism. Soc. Japan *2*, 331.

WATANABE, H. (1971), *Determination of Earthquake Magnitude at Regional Distance in and near Japan*, Zisin (Bull. Seism. Soc. Japan) *32*, 281–296. (in Japanese with an English abstract).

WIEMER, S., *Analysis of Seismicity: New Techniques and Case Studies*, Dissertation Thesis (University of Alaska, Fairbanks, Alaska 1996) 151 pp.

WIEMER, S., and WYSS, M. (1994), *Seismic Quiescence before the Landers ($M = 7.5$) and Big Bear ($M = 6.5$) 1992 Earthquakes*, Bull. Seismol. Soc. Am. *84*, 900–916.

WYSS, M. (1986), *Seismic Quiescence Precursor to the 1983 Kaoiki ($M_s = 6.6$), Hawaii Earthquake*, Bull. Seismol. Soc. Am. *76*, 785–800.

WYSS, M., KLEIN, F. W., and JOHNSTON, A. C. (1981), *Precursors to the Kalapana $M = 7.2$ Earthquake*, J. Geophys. Res. *86*, 3881–3900.

WYSS, M., HABERMANN, R. E., and GRIESSER, J. C. (1984), *Seismic Quiescence and Asperities in the Tonga-Kermadec Arc*, J. Geophys. Res. *89*, 9293–9304.

WYSS, M., and BURFORD, R. O. (1985), *Current Episodes of Seismic Quiescence along the San Andreas Fault between San Juan Baustista and Stone Canyon, California: Possible Precursors to Local Moderate Mainshocks*, U.S. Geol. Survey Open-file Report *85–754*, 367–426.

WYSS, M., and BURFORD, R. O. (1987), *A Predicted Earthquake on the San Andreas Fault, California*, Nature *329*, 323–325.

WYSS, M., and HABERMANN, R. E. (1988), *Precursory Quiescence before the August 1982 Stone Canyon, San Andreas Fault, Earthquake*, Pure appl. geophys. *126*, 333–356.

WYSS, M., SHIMAZAKI, K., and URABE, T. (1996), *Quantitative Mapping of a Precursory Quiescence to the Izu-Oshima 1990 ($M = 6.5$) Earthquake, Japan*, Geophys. J. Int. *127*, 735–743.

WYSS, M., and MARTIROSYAN, A. H. (1999), *Seismic Quiescence before the $M = 7$, 1988, Spitak Earthquake, Armenia*, submitted to GJI.

(Revised October 14, 1998, revised January 4, 1999, accepted January 22, 1999)